Protein Science (1995), *4*:1730–1742. Cambridge University Press. Printed in the USA.

The structure of human pancreatic α-amylase at 1.8 Å resolution and comparisons with related enzymes

GARY D. BRAYER,[1] YAOGUANG LUO,[1] AND STEPHEN G. WITHERS[1,2]

[1] Department of Biochemistry and Molecular Biology and [2] Department of Chemistry, University of British Columbia, Vancouver, British Columbia V6T 1Z3, Canada

(RECEIVED March 22, 1995; ACCEPTED June 30, 1995)

Abstract

The structure of human pancreatic α-amylase has been determined to 1.8 Å resolution using X-ray diffraction techniques. This enzyme is found to be composed of three structural domains. The largest is Domain A (residues 1–99, 169–404), which forms a central eight-stranded parallel β-barrel, to one end of which are located the active site residues Asp 197, Glu 233, and Asp 300. Also found in this vicinity is a bound chloride ion that forms ligand interactions to Arg 195, Asn 298, and Arg 337. Domain B is the smallest (residues 100–168) and serves to form a calcium binding site against the wall of the β-barrel of Domain A. Protein groups making ligand interactions to this calcium include Asn 100, Arg 158, Asp 167, and His 201. Domain C (residues 405–496) is made up of antiparallel β-structure and is only loosely associated with Domains A and B. It is notable that the N-terminal glutamine residue of human pancreatic α-amylase undergoes a posttranslational modification to form a stable pyrrolidone derivative that may provide protection against other digestive enzymes. Structure-based comparisons of human pancreatic α-amylase with functionally related enzymes serve to emphasize three points. Firstly, despite this approach facilitating primary sequence alignments with respect to the numerous insertions and deletions present, overall there is only ~15% sequence homology between the mammalian and fungal α-amylases. Secondly, in contrast, these same studies indicate that significant structural homology is present and of the order of ~70%. Thirdly, the positioning of Domain C can vary considerably between α-amylases. In terms of the more closely related porcine enzyme, there are four regions of polypeptide chain (residues 237–250, 304–310, 346–354, and 458–461) with significantly different conformations from those in human pancreatic α-amylase. At least two of these could play a role in observed differential substrate and cleavage pattern specificities between these enzymes. Similarly, amino acid differences between human pancreatic and salivary α-amylases have been localized and a number of these occur in the vicinity of the active site.

Keywords: amylase; crystallography; enzymology; glycogen; pancreatic; sequences; starch; structure

α-Amylases catalyze the hydrolysis of α-1,4 glucan linkages in starch and are widely distributed in nature, being found in bacteria, plants and animals. In humans, α-amylase is composed of 496 amino acids in a single polypeptide chain, which is encoded on chromosome 1 as part of a multigene family (Gumucio et al., 1988). These genes are regulated so that different isozymes are synthesized in either salivary glands or the pancreas. The salivary and pancreatic α-amylases are highly homologous in terms of primary sequence (Nishide et al., 1986) but do exhibit somewhat different cleavage patterns (Minamiura, 1988). The functional differences observed undoubtedly arise from the 15 amino acid substitutions between these sequences, some of which occur in the putative active site region.

The digestion of starch occurs in several stages in humans (Truscheit et al., 1981; Semenza, 1987). Initially salivary α-amylase provides a partial digestion, which breaks down polymeric starch into shorter oligomers. Upon reaching the gut this partially digested starch is then extensively hydrolyzed into smaller oligosaccharides by the α-amylase synthesized in the pancreas and excreted into the lumen. The resultant mixture of oligosaccharides, including maltose, maltotriose, and a number of α-(1–6) and α-(1–4) oligoglucans, then passes through the mucous layer to the brush border membrane. At this point a number of α-glucosidases function to further degrade the oligosaccharides to glucose. This glucose is then absorbed and enters the bloodstream by means of a specific transport system.

Reprint requests to: Gary D. Brayer, Department of Biochemistry and Molecular Biology, University of British Columbia, Vancouver, British Columbia V6T 1Z3, Canada; e-mail: usergbbc@mtsg.ubc.ca.

An unusual feature of α-amylases isolated from different sources is the substantial divergence observed in their primary sequences. Only minimal homology is observed in sequence alignments and this is restricted for the most part to four short segments (4–9 residues in length) of polypeptide chain (Nakajima et al., 1986; MacGregor, 1988; Jespersen et al., 1993). In contrast, structural studies on a limited number of these enzymes have shown that greater homology exists between them with respect to polypeptide chain folding. α-Amylase structures completed thus far include those of barley (Kadziola et al., 1994), pig (Qian et al., 1993; Larson et al., 1994) and the fungal enzymes from *Aspergillus oryzae* (Swift et al., 1991) and *Aspergillus niger* (Brady et al., 1991). These results also show that these α-amylases have similar active site regions that are centered about three highly conserved carboxylate groups. However, although some progress has been made in understanding the roles of these residues in the catalytic event mediated by α-amylase (Qian et al., 1994), much of this process remains poorly understood.

Our current work concerns gaining a better understanding of the function of human pancreatic α-amylase through elucidation of the three-dimensional structure of this enzyme using X-ray diffraction techniques. With these structural analyses the dual objectives of determining the overall polypeptide chain fold of human pancreatic α-amylase and attaining an accurate assessment of the active site architecture of this enzyme can be achieved. These data will assist future studies in the rational design of inhibitory agents that present therapeutic opportunities in a number of areas, including the control of diabetes, hyperlipoproteinemia, and possibly obesity (Truscheit et al., 1981; Clissord & Edwards, 1988; Brogard et al., 1989; Scheppach et al., 1989). These studies also allow for comparisons of the structure of human pancreatic α-amylase with those of its counterparts from different organisms. The sequence, structure, and function differences observed between these α-amylases present a further opportunity to gain insight into the details of the catalytic mechanism utilized by this family of enzymes.

Results

A schematic representation of the overall polypeptide chain fold determined for human pancreatic α-amylase is shown in Figure 1, along with the locations of each of the bound calcium and chloride ions. In total this protein is composed of three structural domains. The largest is Domain A, which consists of an eight-stranded parallel β-barrel surrounded by a concentric cylinder of α-helical segments. The direction of view in Figure 1 is set so as to look directly down on the top of the β-barrel of Domain A, where the three putative active site residues Asp 197, Glu 233, and Asp 300 are located. Also bound near to the active site is the chloride ion. An interesting feature of Domain A is that it is constructed from two segments of polypeptide chain that include residues 1–99 and 169–404.

Domain B is constructed from residues 100–168, which occur between the third β-strand and α-helix of the central β-barrel of Domain A. It primarily forms β-structure, although a small helix is present. The folding of Domain B forms a pocket against the wall of the β-barrel of Domain A in which the bound calcium ion is found. As evident in Figure 2, the overall thermal factors for main-chain atoms in Domain B (32.0 Å^2) are considerably higher than those of Domains A (17.3 Å^2) and C (20.5 Å^2). These results suggest one role of the calcium binding site of human α-amylase is to stabilize the structure of Domain B.

Domain C is made up of residues 405–496 and forms a compact unit on the opposite side of Domain A from Domain B. As

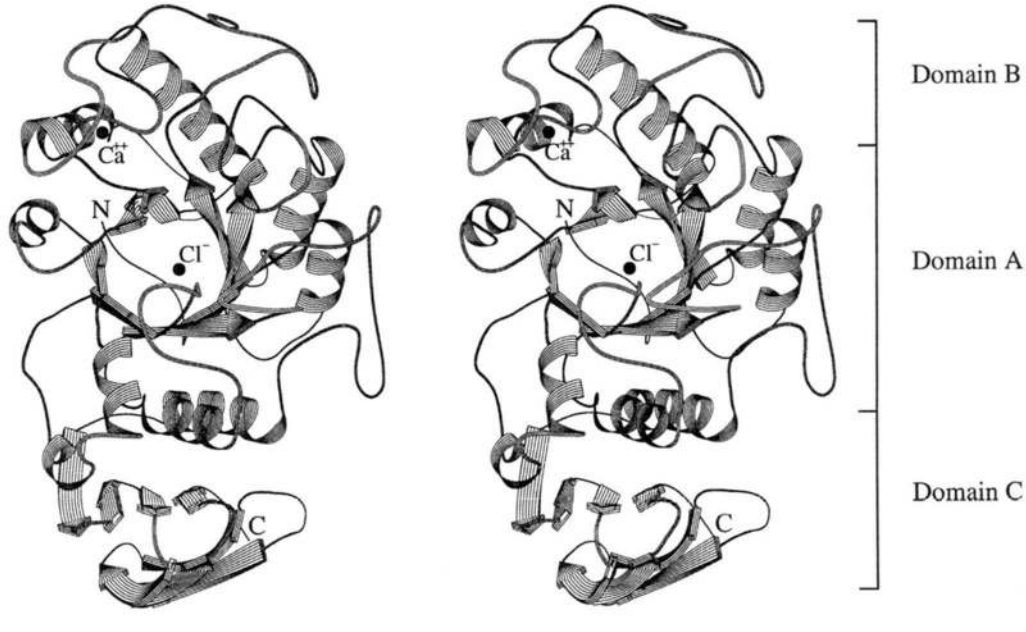

Fig. 1. Stereo drawing of a schematic representation of the polypeptide chain fold of human pancreatic α-amylase. Also indicated are the relative positionings of the three structural domains present in this protein (Domain A, residues 1–99, 169–404; Domain B, residues 100–168; Domain C, residues 405–496), along with locations of the calcium and chloride binding sites. N- and C-terminal ends of the polypeptide chain have also been labeled N and C, respectively. A central feature of this structure is the eight-stranded parallel β-barrel that forms the bulk of Domain A and is believed to contain the active site region.

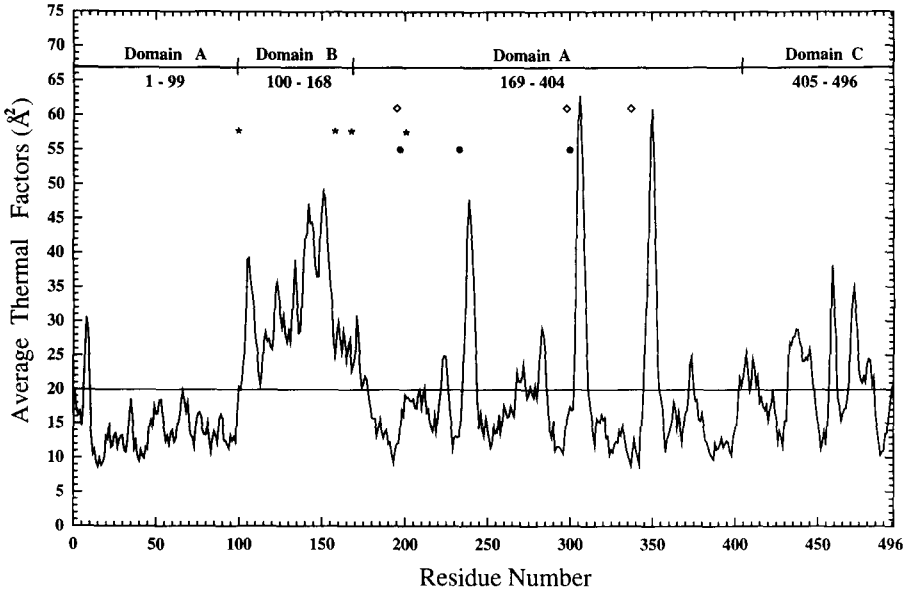

Fig. 2. A plot of the average thermal factors of main-chain atoms along the polypeptide chain of human pancreatic α-amylase. The horizontal line drawn at 20.0 Å^2 represents the average value for the thermal factors of all main-chain atoms. At the top of this plot is an indication of how this protein is divided into domains and the locations within the polypeptide chain where residues involved in calcium (*) and chloride (◇) ion binding are located, along with those believed to play a direct role in catalysis (●). It is clearly evident that Domain B as a whole has significantly higher main-chain thermal factors, with an overall average of 32.0 Å^2. This is in contrast to the average values of 17.3 Å^2 and 20.5 Å^2 found for Domains A and C.

can be seen in Figure 1, Domain C folds into an antiparallel β-barrel type structure and is overall much more loosely associated with Domain A than is seen for Domain B. In terms of primary sequence, it is Domain C that is found to be the most variable between α-amylases of different origins (MacGregor, 1988; Jespersen et al., 1993).

One unique structural feature of human pancreatic α-amylase occurs at its N-terminal end. Here the side-chain CD carbon atom of the terminal glutamine residue is covalently bonded back to the normally free terminal main-chain amino group to form a stable pyrrolidone derivative (pyrrolid-2-one-5-carboxylic acid). This posttranslational modification is believed to occur spontaneously (Kluh, 1981; Bodansky & Martinez, 1983) and results in the loss of the terminal ND2 amide nitrogen group of the side chain of Gln 1 in the form of NH_3. Figure 3 shows the conformation of the polypeptide chain in the vicinity of Gln 1 and Tyr 2, and the unusual N-terminal end structure formed. Despite their exposed surface positioning, these residues are found to be well ordered with an average thermal factor for all atoms of 18.4 Å^2. This is also apparent from the well-defined omit map difference electron density found in the vicinity of these residues as shown in Figure 3. This unusual N-terminal structure may be a defensive mechanism against amino-peptidases and other digestive enzymes that are present in the medium in

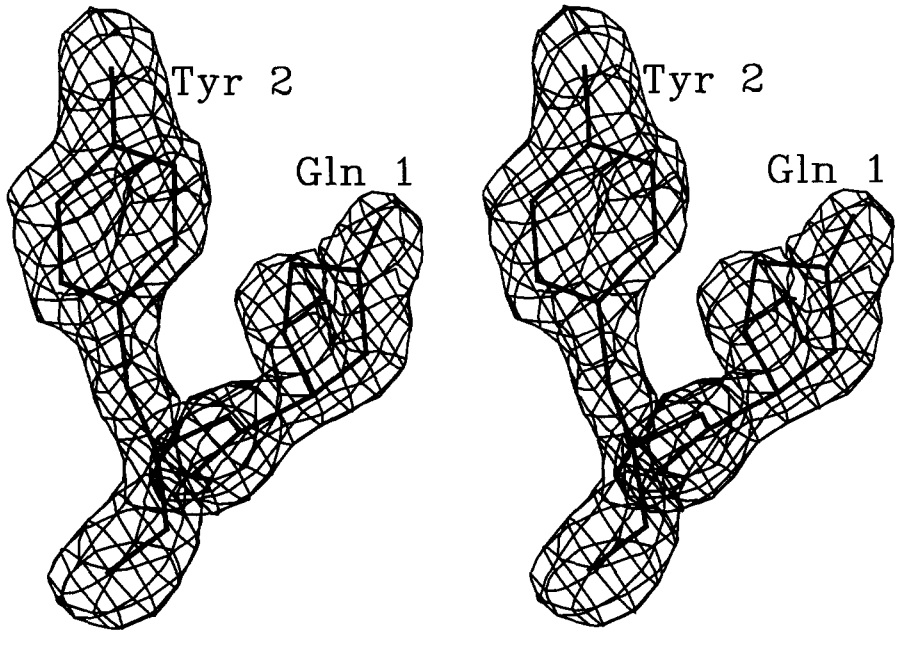

Fig. 3. Stereo diagram of an omit difference electron density map in the region of the N-terminal end of the polypeptide chain of human pancreatic α-amylase. This map was computed with the omission of the whole of Gln 1 and Tyr 2, and the contoured envelope is shown at the 4σ level. Overlaid in dark lines are the final refined positions of Gln 1 and Tyr 2. As can be seen from these results, in human α-amylase the side chain of Gln 1 is covalently bonded back to what would normally be the free terminal amino group of this residue to form a stable pyrrolidone derivative.

which human α-amylase must function. It is notable that all primary sequences of mammalian α-amylases appear to have an N-terminal glutamine residue (Toda, 1988).

Early in our structural analyses of human pancreatic α-amylase, and before it was recognized that Gln 1 formed a pyrrolidone derivative, attempts were made to fit this residue into electron density maps as a normal glutamine. This led to unsatisfactory stereochemistry and abnormally high thermal factors for the side-chain atoms of this residue. It is of interest that in both structure determinations of porcine α-amylase (Qian et al., 1993; Larson et al., 1994) Gln 1 was refined as a normal amino acid. In both cases considerable disorder, coupled with high thermal factors, were noted for Gln 1 and Tyr 2. These results and our observations with human pancreatic α-amylase (Fig. 3) suggest the porcine enzyme, like its human counterpart, also has a cyclic pyrrolidone end and that each of these porcine structures should be reexamined to see if this feature would better fit the observed electron density. The results of an earlier primary sequence analysis have also suggested that Gln 1 in porcine α-amylase is a pyrrolidone derivative (Kluh, 1981).

With few exceptions, the observed electron density over the course of the polypeptide chain of human α-amylase was comparable to that shown for Gln 1 and Tyr 2 in Figure 3. The only extended region having weak electron density for main-chain atoms consisted of residues 304–309, which are part of a flexible surface loop. As Figure 2 shows, these residues have correspondingly high thermal parameters, the average of which for main-chain atoms is 51.7 Å^2, as compared to 20.0 Å^2 for all main-chain atoms. In particular, no significant electron density was observed for Gly 306. This region of polypeptide chain is near the active site residue Asp 300 and may play a role in binding to substrates (Qian et al., 1994). Two other segments of polypeptide chain (residues 236–244 and 346–353) exhibit elevated thermal factor values. Both of these are part of extended loops, with one being adjacent to another active site residue (Glu 233). The positions of a number of side chains belonging to solvent-exposed amino acids were also not clearly defined. Residues having only weak electron density beyond CB include Gln 8, Asn 105, Trp 134, Gln 234, Asn 350, Asn 459, and Asp 471. Those poorly resolved beyond CG were lysines 142, 208, 243, 278, 322, and Arg 343.

Two other notable features of human pancreatic α-amylase are its ability to bind a chloride and calcium ion. As Figure 1 shows, the chloride ion is bound in the direct vicinity of the active site and may serve as an allosteric activator of catalysis (Levitzki & Steer, 1974; Lifshitz & Levitzki, 1976). Chloride ion coordination involves the side chains of Arg 195, Asn 298, and Arg 337, along with a water molecule. These interactions are illustrated in Figure 4A and Kinemage 4, with the corresponding distances involved detailed in Table 1. Two of the chloride ion ligands observed (Arg 195 and Asn 298) are adjacent to active site residues (Asp 197 and Asp 300). This chloride ion is well resolved in electron density maps and has a thermal factor of 31.0 Å^2.

The overall positioning of the bound calcium ion in human pancreatic α-amylase is shown in Figure 1 and its immediate environment is illustrated in Figure 4B and Kinemage 3. A total of eight ligand interactions are made from main-chain, side-chain, and water molecules to this calcium ion and the distances involved are listed in Table 2. This calcium ion is tightly bound (Vallee et al., 1959) and refines to a thermal factor of 20.8 Å^2.

Table 1. *Chloride ion binding site interactions in human and porcine α-amylases*

		Distances (Å)	
Interaction	Atom	Human	Porcine
Arg 195	NE	3.47	3.27
	NH2	3.32	3.37
Asn 298	ND2	3.25	3.26
Arg 337	NH1	3.35	3.39
	NH2	3.16	3.06
Wat	O	3.32	3.21

With the exception of the interaction to the Domain A residue His 201, all others from calcium to protein groups involve amino acids in Domain B. In many respects, the calcium binding site is a central organizing structural feature of Domain B, the polypeptide chain of which wraps itself around this site. It also serves to bind Domain B to the surface of Domain A in the vicinity of the substrate binding channel (Qian et al., 1994). It has been shown that the presence of calcium is essential for catalytic activity (Vallee et al., 1959).

Other polypeptide chain features of note in human α-amylase include Ser 414 and the two *cis*-prolines at residues 54 and 130. Ser 414 is the only amino acid that has refined ϕ, ψ angles (−124°, −110°) that fall outside the limits normally observed. Reference to electron density maps shows that Ser 414 is well resolved and is part of the end of an extended surface loop. The terminal turn of this loop is unusual in that hydrogen bonds from the side chain of Asn 412 to the main-chain amide groups of Ser 414 and Gln 416 appear to mediate the curvature of this turn. A further hydrogen bond from the side chain of Asn 415 is formed to the side chain of Ser 414. Thus, it appears that the unusual hydrogen bonds formed in this turn are responsible for the nonstandard main-chain torsional angles of Ser 414. Both of *cis*-prolines 54 and 130 are also located at the ends of extended β loops. Each of these is well resolved in electron density

Table 2. *Calcium ion binding site interactions in human, porcine, and the fungal α-amylases from Aspergillus oryzae (Taka) and niger (Niger)*

		Distances (Å)			
Interaction[a]	Atom	Human	Porcine	Taka	Niger
Asn 100 (Asp)	OD1	2.31	2.31	2.63	2.56
Arg 158 (Glu)	O	2.51	2.32	2.55	2.63
Asp 167	OD1	2.58	2.67	2.66	2.81
	OD2	2.49	2.64	2.74	2.61
His 201 (Glu)	O	2.41	2.28	2.63	2.40
Wat	O	2.46	2.44	2.36	2.50
Wat	O	2.49	2.49	2.43	2.58
Wat	O	2.65	2.62	2.67	2.60

[a] Residue numbering is according to the sequence alignment of Figure 5, with amino acids differing from those of human α-amylase indicated in brackets.

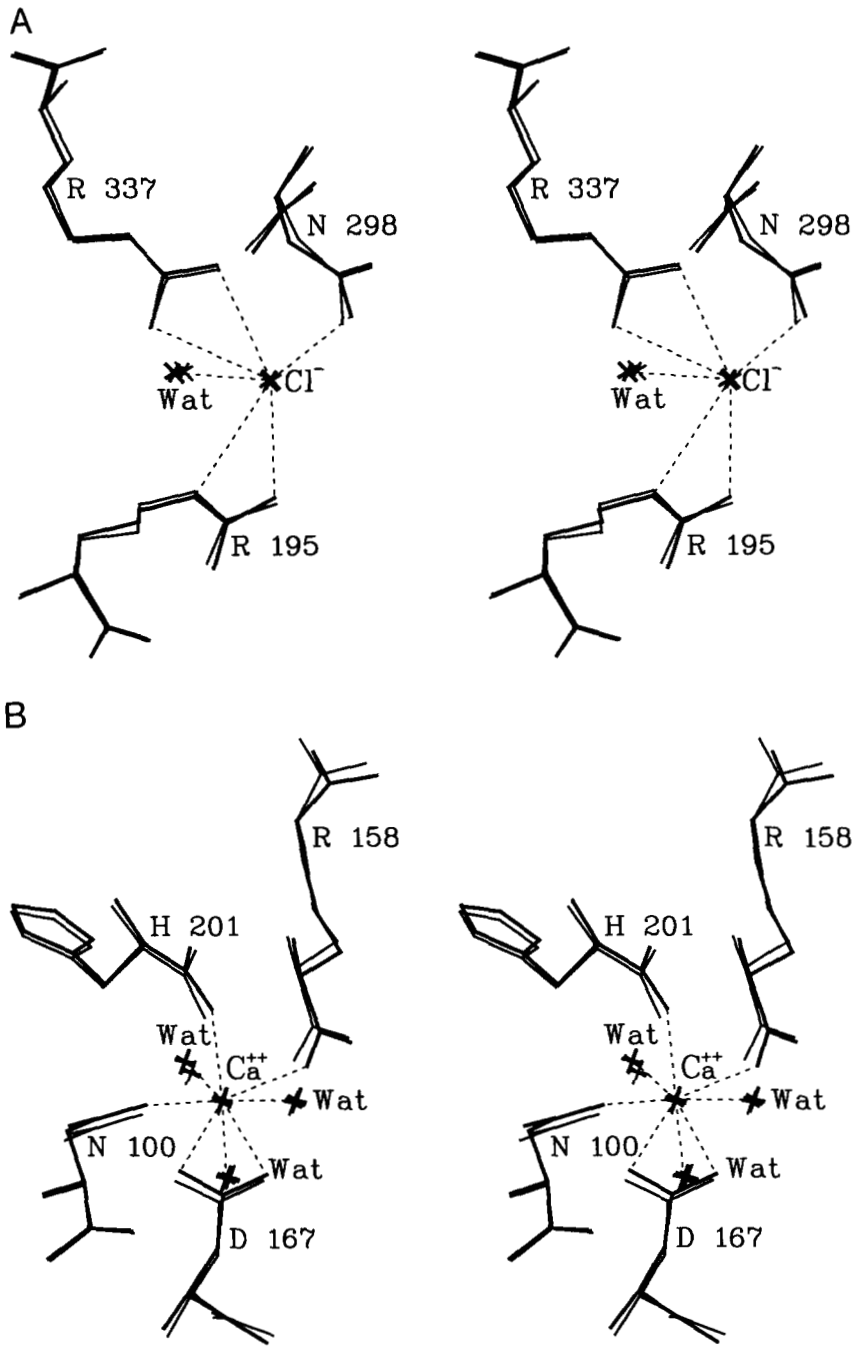

Fig. 4. Stereo drawings showing the coordination sphere of the **(A)** chloride ion bound to human (thick lines) and porcine (thin lines) pancreatic α-amylases, as well as **(B)** the calcium ion bound to these enzymes and **(C)** the comparable calcium site found for the fungal Taka (thick lines) and Niger (thin lines) α-amylases. Coordination interactions are indicated with dashed lines and the distances involved are presented in Tables 1 and 2. Bound water molecules have also been drawn and labeled "Wat." Amino acid numbering is according to the alignment presented in Figure 5. (*Continues on facing page.*)

maps and appears to have been placed to assist in the execution of the sharp turns necessary in the polypeptide chain at these positions.

Discussion

Primary sequence alignments

One remarkable feature of α-amylases isolated from different sources is the divergence observed in their primary sequences. For example, alignments of the sequences of animal and fungal α-amylases has found homology on the order of only ~10% between the residues present. Indeed, the dissimilarity between the sequences determined for members of this family of enzymes has made formulating justifiable alignments of these very difficult, with the necessity of introducing multiple insertions and deletions at arbitrary positions to achieve even minimal correspondence (for example, see MacGregor, 1988; Jespersen et al., 1993).

Overall such studies have found only four short segments of polypeptide chain that demonstrate reasonably good homology amongst the α-amylases. These include residues 96–101, 193–201, 233–236, and 294–301 (Fig. 5). The first of these segments is involved in binding a calcium ion, whereas the latter three each

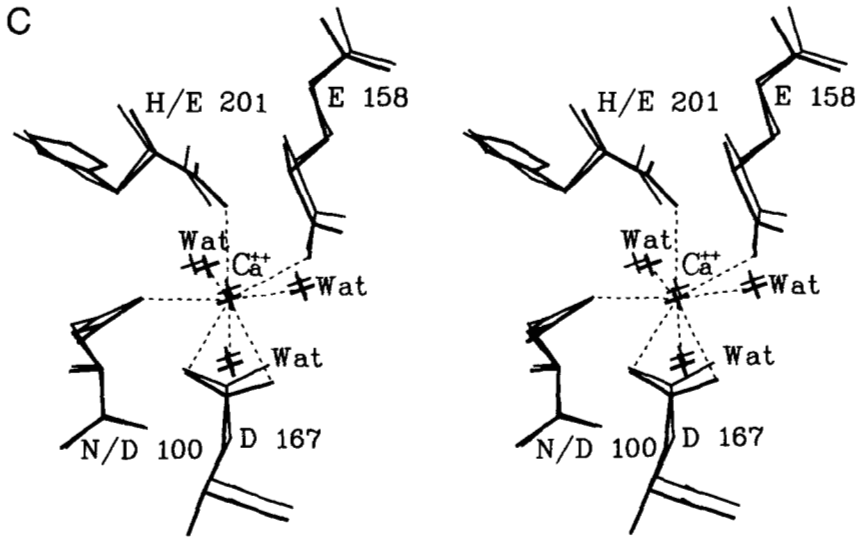

Fig. 4. *Continued*

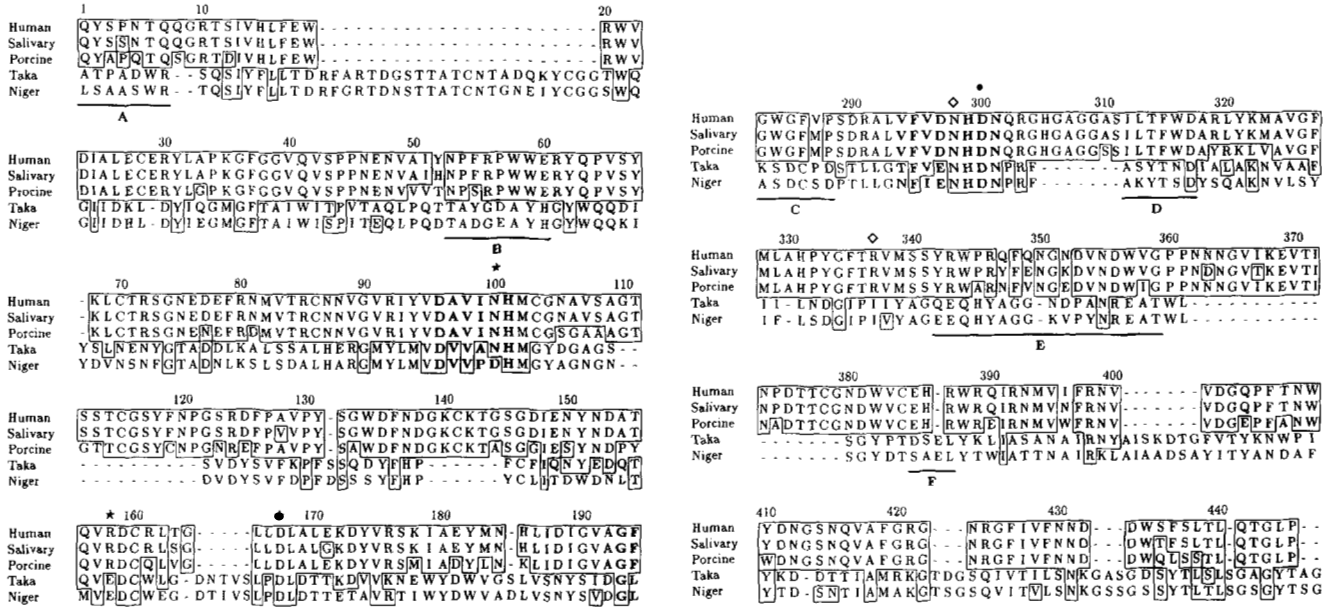

Fig. 5. Sequence comparison of human pancreatic and salivary, porcine, Taka, and Niger α-amylases. Sequences of human pancreatic (Nakamura et al., 1984; Wise et al., 1984; Nishide et al., 1986) and salivary (Nakamura et al., 1984; Nishide et al., 1986), porcine (Pasero et al., 1986; Qian et al., 1993), Taka (Toda et al., 1982), and Niger (Takkinen et al., 1983) α-amylases have been aligned so as to maximize the structural homology present. The single-letter code is used to identify amino acids and the residue numbering is based on the sequence of human pancreatic α-amylase. Primary sequence identity with that of the human pancreatic enzyme is indicated by the boxes drawn. Also indicated are residues involved in forming the calcium (*) and chloride (◇) binding sites, as well as those residues (●) believed to directly take part in the catalytic mechanism of α-amylase. Four short segments of polypeptide chain that are highly conserved in all α-amylases are printed in bold. Portions of polypeptide chain that occur at the same primary sequence location in this figure but that are found to fold in different conformations between the mammalian and fungal α-amylases are heavily underlined and labeled with the letters A–H. The precise locations of these structurally different polypeptide chain segments in the three-dimensional structures of human pancreatic and Taka α-amylases are indicated in Figure 6.

contain a putative active site residue (Boel et al., 1990; Larson et al., 1994; Qian et al., 1994). In total, these represent 27 amino acids out of the ~500 that make up the typical α-amylase. All other regions of the polypeptide chain sequences of animal and fungal α-amylases have essentially no homology when aligned using traditional methods based on matching schemes dependent solely on amino acid identity.

Despite the results obtained from sequence alignments, recent structural studies have shown that α-amylases do have considerable similarity with regard to polypeptide chain folding. With the availability of the atomic coordinates for the porcine (Larson et al., 1994), Taka (Swift et al., 1991), and Niger (Brady et al., 1991) α-amylases, along with those of the human pancreatic enzyme as determined in this study, it is now possible to take a structure-based approach to facilitate a more accurate sequence alignment for these α-amylases. We have completed such a study and the results are presented in Figure 5. In this work an optimal spatial overlap between the different α-amylases was achieved by a least-squares fit of main-chain atoms of those residues in the four homologous primary sequence segments present, in addition to the position of the bound calcium ion and the main-chain atoms of those residues with which it interacts (29 residues in total).

Figure 6A and Kinemage 1 show the structural overlap achieved for Domains A and B by this approach for the human and Taka α-amylases. It is clear from these results that there is a high degree of structural homology between these enzymes and a similar result is obtained when comparisons are made between these and the porcine and Niger enzymes as well. Reference to such diagrams has allowed a topological assessment of the true alignment of the primary sequences of these α-amylases (Fig. 5). Of particular value in these studies was the ability to use structural correspondence to place the variety of differing length insertions and deletions in sequence that occur between these enzymes. The patterns of insertions and deletions observed in our studies are significantly different than those derived from sequence-based alignments (Nakajima et al., 1986) and could serve to appropriately position the corresponding segments in the sequences of α-amylases for which structures are still unavailable.

A difficulty encountered in these structural comparisons involved Domain C (residues 405–496) and the segment of polypeptide chain (residues 340–404) linking it to Domain A. Domain C appears to be only loosely linked to the core of α-amylase formed by Domains A and B and has a substantially shifted overall positioning in the fungal enzymes. Thus, despite having a comparable overall fold in all four enzymes, it could not be properly aligned as described above. Also presenting a difficulty is the fact that there are no discernible segments of primary sequence homology in Domain C that might form the basis for overlapping this structural element between different α-amylases.

To resolve this problem, the best structural overlap between the human, Taka, and Niger α-amylase structures based on Domains A and B was taken as an initial starting point. Then the polypeptide chain of the Taka and Niger structures was artificially cleaved at residue 340, which is at the start of the polypeptide chain segment linking Domains A and C. With the aid of a molecular graphics workstation, Domain C of each fungal enzyme was then rotated and translated to achieve the maximal overlap of main-chain coordinates with Domain C of human α-amylase. On this basis, the main-chain atoms of 56 residues dispersed throughout Domain C were identified as being in homologous positions in all three enzymes and used to guide a subsequent least-squares refinement of the initial structural overlaps. It was found that rotations of 21.2° and 24.0°, along with translations of 6.4 Å and 8.0 Å, were required to optimally overlap Domain C of Taka and Niger α-amylases, respectively, onto Domain C of the human enzyme. As Figure 6B shows, this approach allowed for excellent fits of related domains, and as found for Domains A and B, demonstrates the high degree of structural homology present between the mammalian and fungal α-amylases despite the lack of primary sequence homology. As shown in the subsequent alignment of the primary sequences of Domain C based on these structural overlaps (Fig. 5), one feature of this domain is the presence of a relatively large number of insertions and deletions between sequences. Reference to individual α-amylase structures shows these occur for the most part at the surface-exposed ends of β-loops. The fungal enzymes also have notably extended C-terminal ends.

It is clear from a comparison of the structural alignments of sequences presented in Figure 5, with earlier sequence-based alignments (Nakajima et al., 1986; MacGregor, 1988), that these are significantly different. These new results serve to make two points. First, no matter which alignment procedure is used, the overall primary sequence homology observed between α-amylases is found to be low. Thus, the primary sequence identity found by a structure-based approach for Taka (17%) and Niger (14%) α-amylases in comparison to the human enzyme, is only marginally higher than that found by traditional sequence-matching techniques (~10%). A second conclusion is that, despite these sequence alignment results, there is significant structural homology between distantly related α-amylases. For example, our work shows that overall there is ~70% topological equivalence between the animal and fungal groups of α-amylases. This suggests that other α-amylases whose primary sequences are correspondingly dissimilar are also likely to fold into structures comparable to that of human, porcine, Taka, and Niger α-amylases. It seems within the α-amylase family of enzymes, that beyond the four short segments of polypeptide chain related to active site structure, considerable flexibility is available to alter the identities of other residues to optimize enzymatic activity under the particular conditions that each α-amylase is required to function. Thus, for these enzymes, polypeptide chain folding is the overriding constraint over the course of molecular evolution as opposed to preservation of primary sequence identity.

Another surprising result arising from Figure 5 is the presence of eight segments of polypeptide chain that occur at comparable positions in the primary sequences of both the animal and fungal enzymes, but which are found to have very different folding conformations (see Fig. 6 and Kinemages 1 and 2). These segments range in size from 4 to 20 residues and on average contain nine amino acids. Of the 71 residues involved, 62 occur in Domain A, with the remainder found in Domain C. As Figure 5 shows, among these 71 residues, only 4 are conserved in all five primary sequences. The alternative folding observed for two of these segments could be rationalized from the point of view that they occur at the termini of the polypeptide chain. At these locations there are fewer constraints on polypeptide chain folding and therefore the opportunity for greater flexibility in positioning. However, in the case of the other six intrachain seg-

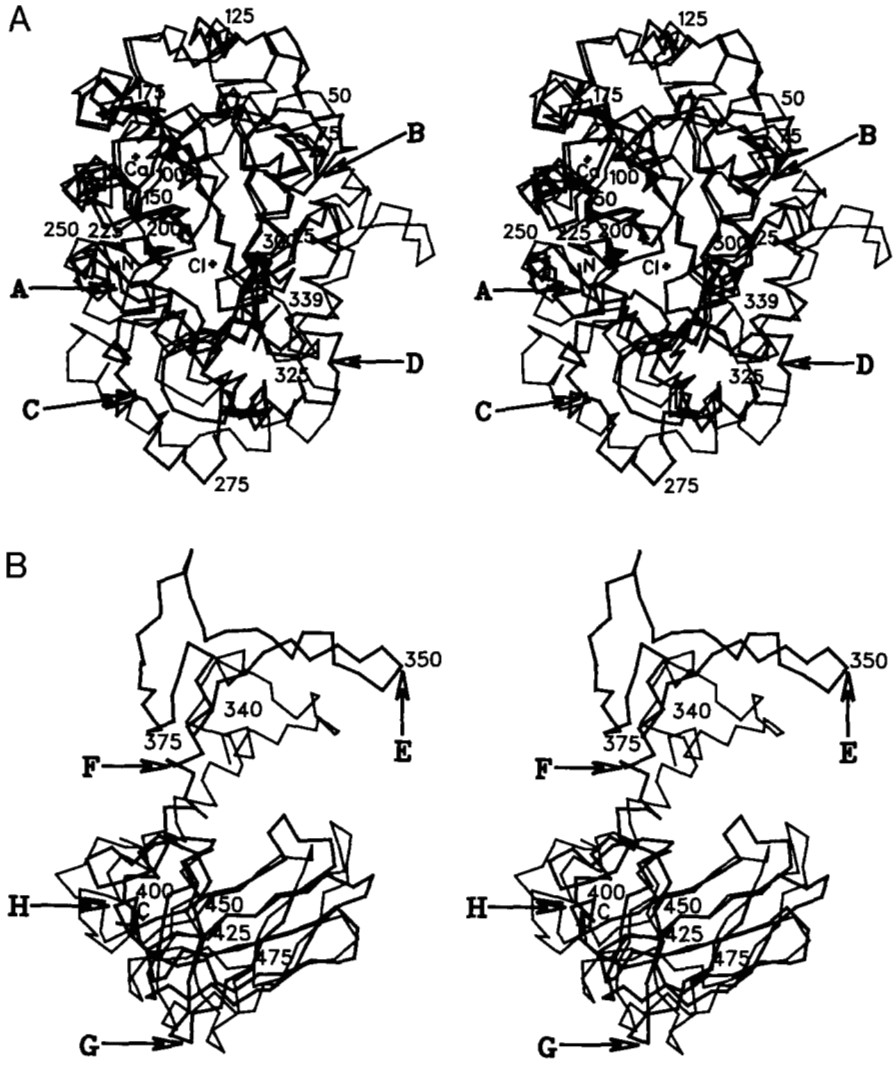

Fig. 6. Stereo drawings of optimized overlaps of the course of the polypeptide chains of (**A**) residues 1–339 and (**B**) residues 340–496 of human (thick lines) and Taka (thin lines) α-amylases. Residues 1–339 comprise Domain B and most of Domain A (Fig. 1). Overlap of these two domains was based on a least-squares fit of the main-chain atoms of residues in four segments of conserved primary sequence between these enzymes, as well as those forming ligands in a common calcium binding site (Table 2). Positions of the calcium and chloride ions bound to human α-amylase are also drawn. Residues 340–496 represent the linker region between Domains A and C, and Domain C itself. Although Domain C has a similar folding topology in the human and Taka α-amylases, it has a different placement with respect to Domains A and B in these enzymes. Structural overlap of Domain C was achieved by cleavage of the polypeptide chain at residue 340, followed by manual and least-squares refinement to achieve the best correspondence as described in the text. These results show that Domain C in Taka α-amylase is rotated and translated by 21.2° and 6.4 Å, with respect to its human counterpart. As described in the text and indicated in Figure 5, there are eight segments of corresponding primary sequence between the mammalian and fungal α-amylases that in fact have very different structural conformations. These are indicated by the arrows and the letters A–H. See Figure 5 for the exact alignment of these segments. The primary sequence numbering shown is that of human pancreatic α-amylase (Fig. 5) and every 25th amino acid along the polypeptide chain has been labeled, along with the terminal ends.

ments, it is less clear what might be promoting alternative polypeptide chain conformations. For the most part these segments consist of extended loops and in their new conformations interact with different surface groups. It is likely that long-range interactions formed by alternative amino acids substituted in other portions of the polypeptide chain dictate the preferential folding of these loops, which have greater freedom of movement than polypeptide chains buried in the core of the enzyme. These results serve to highlight another difficulty in comparing primary sequences of low homology in the absence of structural information.

Homology of ion binding and active site residues

Beyond the considerable polypeptide chain folding homology observed, the α-amylases compared in Figure 5 are also highly homologous in terms of the site of calcium binding near the active site and the conformations of active site residues. As reference to Figure 4 and Kinemage 3 shows, the positioning, binding ligands, and even associated water molecules within this calcium binding site are virtually identical despite the presence of differences in the identities of some of the amino acids involved. This can be explained by the fact that, with the exception of the replacement of Asn 100 for an aspartate in Niger α-amylase, the main-chain atoms of substituted amino acids form interactions to the calcium atom. A comprehensive list of the interactions formed within this calcium binding site in all four α-amylases is given in Table 2. It is notable that the sequence alignment in Figure 5 does indicate higher than background homologies for segments including residues interacting with calcium. This includes residues 157–160 and 165–168, which are not associated with catalytic residues. These results suggest that calcium binding has similar roles in the animal and fungal enzymes in organizing and stabilizing the structure of Domain B. Additional calcium binding sites found in the plant and fungal α-amylases (Boel et al., 1990; Kadziola et al., 1994), but that are absent in the animal enzymes, do not appear to play a primary role in function.

Another important ion binding site in the animal α-amylases is that for chloride, which acts as an allosteric activator (Levitzki & Steer, 1974; Lifshitz & Levitzki, 1976). Coordination of this ion is provided by the side chains of Arg 195, Asn 298, and Arg 337 (Table 1) and the structure of this binding site is shown

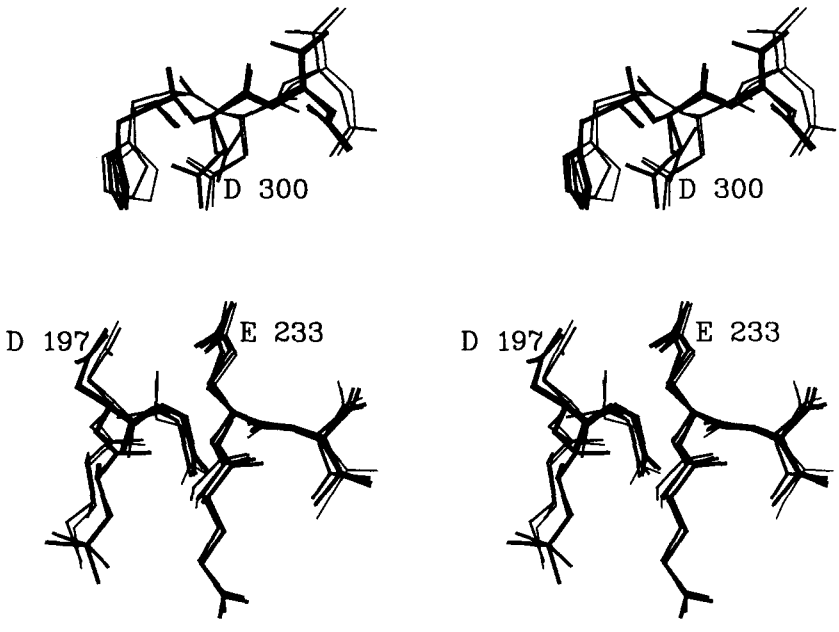

Fig. 7. Stereo drawing showing the similarity in the conformations of the active site residues Asp 197, Glu 233, and Asp 300 in the structures of human, porcine, Taka, and Niger α-amylases. These amino acids and those of immediately surrounding residues in the animal α-amylases are drawn with dark lines, and those from the fungal enzymes are drawn with thin lines. The amino acid numbering scheme used is based on the sequence alignment in Figure 5.

in Figure 4 and Kinemage 4. Reference to Figure 5 shows that two of the amino acids involved are conserved in the fungal enzymes, whereas the third, Arg 337, is replaced by an isoleucine. The absence of chloride binding in the fungal enzymes in light of the similarity of overall polypeptide chain folding in this area with the animal α-amylases points out the importance of the side chain of Arg 337 to chloride binding. It is apparent that the development of enzymatic control afforded by chloride ion is an evolutionarily recent event that does not seem to play a role in enzymes from lower organisms.

Corresponding to the high sequence homology about the active site residues Asp 197, Glu 233, and Asp 300 are very similar conformations for these residues in both animal and fungal α-amylases (Fig. 7 and Kinemage 5). Indeed, three of the most conserved segments of primary sequence in the α-amylases (residues 193–201, 233–236, and 294–301) each contains one of these amino acids. This suggests that, although the particular specificities and cleavage patterns of these α-amylases may vary, the mechanism of catalytic action is likely to be the same. Note that these residues are localized near to the major calcium binding site and in the mammalian enzymes adjacent to the site of chloride binding. A similar constellation of catalytic residues has also been observed in the structure of barley α-amylase (Kadziola et al., 1994).

Human and porcine pancreatic α-amylases

It is of interest to compare the polypeptide chain folding of the human and porcine α-amylases to gain some insight into the differing substrate and cleavage pattern specificities observed between these related mammalian enzymes (for a review see Toda [1988] and references therein). As Figure 5 shows, there are 70 amino acid substitutions between the sequences of these enzymes and these are likely the basis for the functional differences observed. Of the two recent structural determinations of porcine α-amylase, the atomic coordinates for those of Larson et al. (1994) are available and are used herein for structural comparisons.

A plot of the average positional deviations between main-chain atoms in the structures of human and porcine α-amylases is shown in Figure 8. The overall value for all main-chain atoms was found to be 0.32 Å. In total there are four regions of polypeptide chain with significantly different conformations between these enzymes. These include residues 237–250, 304–310, 346–354, and 458–461. The first of these conformational differences is located adjacent to a highly conserved segment of primary sequence (residues 233–236; Fig. 5), which includes the active site residue Glu 233. Four amino acid substitutions occur in this vicinity at residues 241, 245, 246, and 249. Of these, the need to fit a proline in place of an alanine at position 241 in human α-amylase appears to be responsible for the conformational differences observed. Pro 241 also causes the peptide bond between Leu 237 and Gly 238 to flip by ~180° and the course of the polypeptide chain in this region to execute a wider turn than seen in porcine α-amylase. Also affected is the positioning of the α-helix that starts near Pro 241, but substitution of glycine at residue 249 (serine in porcine α-amylase) seems to limit this shift and beyond this latter residue the conformation of the polypeptide chain of both enzymes resumes a similar course. As Figure 2 indicates, overall this region of polypeptide chain has higher thermal parameters than the average.

A second region of conformational differences is also in the active site and involves residues 304–310 (Fig. 8). It follows immediately after a highly conserved segment of primary sequence (residues 294–301) that contains the catalytic residue Asp 300. As shown in Figure 2, the loop formed by residues 304–310 exhibits the highest thermal factors observed in the structure of human α-amylase and much of this flexibility is undoubtedly related to the fact that four of the seven residues involved are glycines. Only one amino acid substitution is present, with Ser 310 of the porcine enzyme becoming alanine in human α-amylase. Although seemingly a small change, residue 310 is directly in the active site region and may be a factor in specificity differences

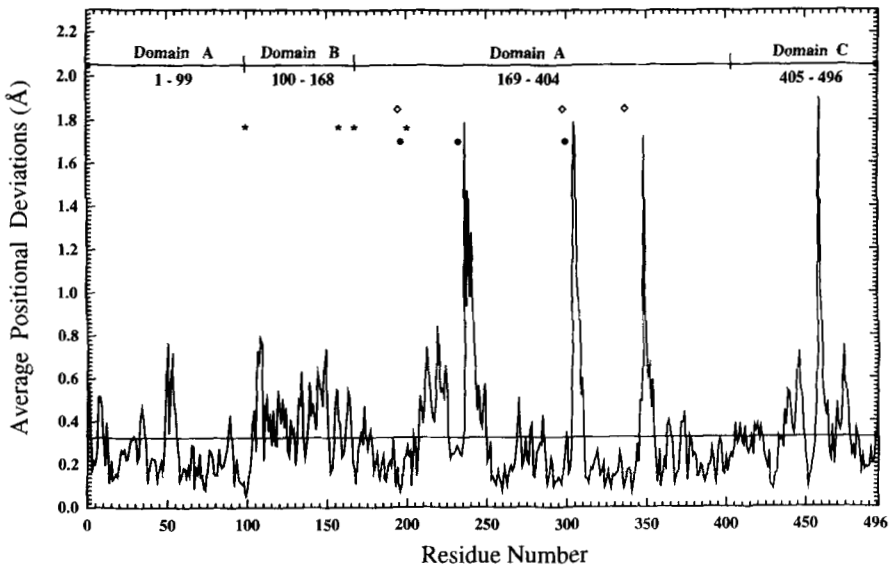

Fig. 8. Plot of the average positional deviations of main-chain atoms between the structures of human and porcine pancreatic α-amylases. The horizontal line drawn represents the overall RMS deviation observed for these atoms of 0.32 Å. At the top of this plot is an indication of how these α-amylases are divided into structural domains and the location of catalytic amino acids (●) and those involved in calcium (*) and chloride (◇) ion binding.

between these enzymes. In porcine α-amylase, this region also has high thermal factors, but, on the binding of an inhibitor in the active site, it becomes much more structured (Qian et al., 1993, 1994). Thus, it appears that the loop formed by residues 304–310 functions by shifting to enhance binding to substrates in the active site as part of catalysis and then moves away to allow for the release of products and the complexation of the next substrate molecule. This would explain not only the multiple conformations observed for this loop between α-amylases but also the high incidence of glycine residues that would facilitate flexibility in the polypeptide chain at this point. It is notable that, with the exception of residue 304, this region of polypeptide chain is deleted from the fungal α-amylases.

A third region of conformational differences between the human and porcine α-amylases occurs in the extended β-loop formed by residues 346–354. This portion of polypeptide chain is part of the link between the A and C domains of these enzymes (Figs. 1, 5 and Kinemages 1 and 2) and exhibits high thermal factors (Fig. 2). A total of three amino acid substitutions are present, involving residues 347, 349, and 352 (Fig. 5). The side chains of Gln 347, Gln 349, Asn 350, and Asn 352 all take on substantially different conformations in human α-amylase, and this is coupled with a flip of the peptide bond between Gln 349 and Asn 350. This new peptide bond conformation results in a new β-turn structure being formed in this region with a hydrogen bond being made between the carbonyl group of Asn 350 and the amide group of Asn 352. As Figure 5 indicates, this portion of polypeptide chain has a substantially different conformation in the fungal α-amylase.

A final region of conformational differences involves residues 458–461, which form an β-turn about midway through Domain C. All four of these residues have different identities in human and porcine α-amylase (Fig. 5). The shifts observed in Figure 8 are likely due to the exchange of glycine and asparagine residues at positions 459 and 460 between these enzyme sequences. Gly 459 is located at the R_2 position of a Type I β-turn in porcine α-amylase. In the human enzyme, Gly 460 is located at the R_3 position, which allows for the formation of a Type II β-turn with a flip of the central peptide bond between residues 459 and 460. The different conformations of Type I and II β-turns accounts for the side-chain shifts observed between human and porcine α-amylase in this region. It is possible that larger differences in structure are avoided due to the stabilizing effect of a local disulfide bridge between residues 450 and 462. Most of this region of polypeptide chain is deleted in the fungal α-amylases (Fig. 5).

Thus, in terms of structural differences, it seems that at least two of four such regions may have an impact on the observed differential substrate and cleavage pattern specificities between human and porcine α-amylases. One of these (residues 237–250) involves multiple mutations in a segment of polypeptide chain adjacent to a highly conserved region of primary sequence containing the catalytic residue Glu 233. Although the structural shifts observed do not affect the placement of Glu 233 (Fig. 7 and Kinemage 5), they could potentially modify local substrate binding preferences. The second region (residues 304–310) is positioned directly in the active site and is known to interact directly with bound substrate. There is one mutation in this area (residue 310) between the human and porcine α-amylase primary sequences, and the conformation of this loop in the absence of substrate is significantly different in these two enzymes (Fig. 8). Whether this conformational difference translates into a different mode of binding to substrates remains to be determined through structural analysis of a substrate or inhibitor complex with human α-amylase. The structural differences observed for the two other portions of polypeptide chain (residues 346–354 and 458–461) that are distant from the active site are less likely to be involved in substrate binding except as part of remote binding interactions with large polymeric substrates.

Human pancreatic and salivary α-amylases

In humans, α-amylase is encoded by a multigene family located on chromosome 1 (Gumucio et al., 1988). The regulation of these genes is such that different α-amylases are expressed in a tissue-specific manner in salivary glands and the pancreas. As is apparent from Figure 5 the primary sequences of the pancreatic and salivary α-amylases are very similar with ~97% homol-

ogy overall. Nonetheless, it has proven possible to develop a monoclonal antibody specific for the pancreatic enzyme (Svens et al., 1989). Functionally the pancreatic and salivary α-amylases have similar but not identical cleavage patterns when tested with a variety of substrates (see review by Minamiura, 1988).

With the determination of the structure of human pancreatic α-amylase the opportunity arises to assess the origin of specificity differences observed in its salivary counterpart. In total there are 15 amino acid differences between the sequences of these two enzymes (Fig. 5). The overall net effect of these substitutions is to add three more polar groups and three additional charged side chains to the salivary α-amylase. The largest concentration of amino acid changes (6 of 15) occurs in the segment of polypeptide chain (residues 340–404) that connects Domains A and C. The number of changes here is comparable to that found in comparisons of the human and porcine pancreatic α-amylases. It is also a region of considerable variance in primary sequence between the mammalian and fungal α-amylase families.

In terms of the active site region, two substitutions in salivary α-amylase could have implications on substrate binding. The first involves the replacement of Thr 163 by a serine. In porcine α-amylase, this residue is believed to interact with bound substrates (Qian et al., 1994). In a second replacement, Leu 196 is exchanged for isoleucine in the middle of a highly conserved region of primary sequence. In the direct vicinity of this substitution are Arg 195, which binds chloride ion, Asp 197, which is a catalytic residue, and His 201, which is part of the calcium binding site. Although the substitutions occurring at residues 163 and 196 are conservative in nature, it is conceivable that changes of this type when located at such strategic positions could have an impact on enzymatic function. Further clarification of the structural elements that lead to differential activity in the human pancreatic and salivary α-amylases will have to await the structural determination of the latter enzyme.

Materials and methods

Human pancreatic α-amylase was isolated and purified from pancreatic tissue using a glycogen affinity precipitation procedure (Loyter & Schramm, 1962; Burk et al., 1993). Crystals of this protein were obtained using the hanging drop method. Crystallizations were preceded by dialyzing the protein solution against 1 mM NH_4OH and 100 mM cacodylate buffer, pH 7.5, to a final concentration of 20 mg/mL. The crystallization reservoir well solution contained 60% 2-methylpentan-2,4 diol. Hanging drops of 10 μL total volume were prepared from 5 μL of the protein solution mixed with 5 μL of reservoir solution. Crystal growth plates were maintained at 22 °C. Crystals of human pancreatic α-amylase are of the space group $P2_12_12_1$, with unit cell dimensions of $a = 53.04$ Å, $b = 74.80$ Å, and $c = 137.34$ Å, with one molecule per asymmetric unit. In total, three crystals were used to collect diffraction intensity data on both Enraf-Nonius FAST and Rigaku R-AXIS II area detectors to 1.8 Å resolution. Details of diffraction data collection and processing are summarized in Table 3.

A molecular replacement approach (XPLOR; Brünger, 1992) was used to position a preliminary model of human pancreatic α-amylase within its unit cell. This starting model consisted of the structure of porcine α-amylase (Larson et al., 1994) in which residues differing between the porcine and human enzymes were modelled as alanines. It was initially centered at the origin of a P1 unit cell with $a = b = 200$ Å, $c = 300$ Å and $\alpha = \beta = \gamma = 90°$, and structure factors were calculated to 4.0 Å resolution. A rotation function search was conducted with the radius of the search limited to 45 Å about the Patterson origin and origin removal applied. The highest peak observed was 10σ above background, with the next highest peak being of height 1σ. After optimization of the rotation function maximum, a three-dimensional translation function search was conducted with data in the same resolution range. The height of the largest peak found in this translation search was 23σ above background. The preliminary solution obtained from the results of the rotation and translation searches was further subjected to rigid body refinement, which resulted in a crystallographic R-factor of 32.9% for data in the 8.0–3.0 Å resolution range. This was followed by individual atomic positional and thermal factor refinement carried out with a data set extended to 2.5 Å resolution. The R-factor was 26.2% at this point. These refinements and all those subsequently were carried out using data such that $F > 2\sigma F$.

Following this preliminary refinement, $2F_o - F_c$, $F_o - F_c$, and omit difference electron density maps were calculated in the regions about those amino acids of human pancreatic α-amylase that had been initially modelled as alanines during molecular replacement searches. Examination of these maps allowed placement of the appropriate side chains missing from the initial refinement model. Subsequent positional and thermal factor refinement, followed by simulated annealing refinement (Brünger, 1990) employing a slow cooling protocol that started at

Table 3. *Data collection and refinement parameters*

I. Data collection	
Space group	$P2_12_12_1$
Cell dimensions (Å)	
a	53.04
b	74.80
c	137.34
Resolution range (Å)	36.1–1.8
No. of unique reflections collected	42,316
Overall completeness(%)	82.1
Inner shell (36.1–2.0 Å)	89.0
Outer shell (2.0–1.8 Å)	63.1
Merging R-factor (%)[a]	5.5
II. Refinement	
No. of reflections used	41,646
Resolution range (Å)	8.0–1.8
No. of protein atoms	3,946
No. of solvent molecules	359
Average thermal factors (Å^2)	
Protein atoms	21.1
Solvent atoms	40.6
Final refinement R-factor (%)[b]	17.4

[a] $$R_{merge} = \frac{\sum_{hkl}\sum_{i=1}^{n} |F_{i_{hkl}} - \bar{F}_{hkl}|}{\sum_{hkl}\sum_{i=1}^{n} F_{hkl}}.$$

[b] $$R_{cryst} = \frac{\sum_{hkl} |F_o - F_c|}{\sum_{hkl} |F_o|}.$$

Table 4. *Stereochemistry of refined human pancreatic α-amylase*

Stereochemical parameter	RMS deviation from ideal values	Restraint weight
Distances (Å)		
Bond (1-2)	0.016	0.016
Angle (1-3)	0.036	0.025
Planar (1-4)	0.049	0.050
Planes (Å)	0.008	0.010
Chiral volumes (Å^3)	0.122	0.080
Nonbonded contacts(Å)		
Single torsion	0.181	0.150
Multiple torsion	0.132	0.150
Possible hydrogen bond	0.135	0.150
Torsion angles (°)		
Planar (0° or 180°)	1.9	2.5
Staggered (±60°, 180°)	16.7	20.0
Orthonormal (±90°)	32.7	15.0

4,000 K, reduced the R-factor to 22.4%. At this stage further $2F_o - F_c$ and $F_o - F_c$ difference electron density maps were calculated, along with a complete set of omit maps in which 10 amino acids were removed sequentially over the entire course of all 496 residues in the polypeptide chain. In this manner, extensive manual refitting of several sections of polypeptide chain was carried out and the calcium and chloride ions were added to the refinement model. Two further rounds of positional, thermal factor, and simulated annealing refinements were then conducted in conjunction with difference electron density maps and manual refittings to give a final R-value of 15.9%. Extension of this structural determination to 1.8 Å resolution followed the same refinement and refitting procedures outlined above. The R-factor at this point in refinement was 19.9%.

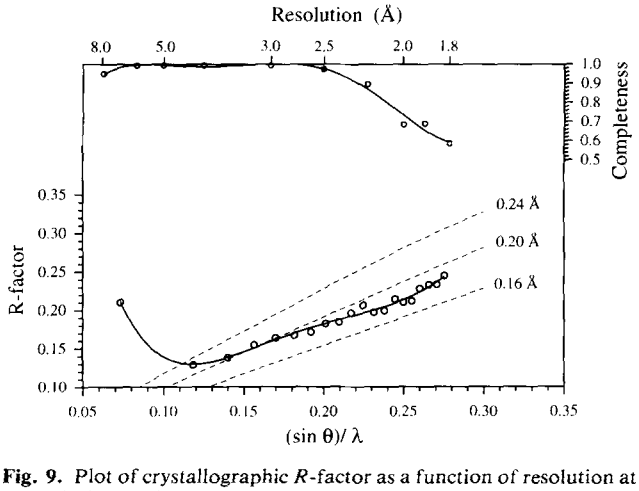

Fig. 9. Plot of crystallographic R-factor as a function of resolution at the end of the refinement of human pancreatic α-amylase. The theoretical dependence of R-factor on resolution assuming various levels of RMS error in the atomic positions of the model (Luzzati, 1952) is shown as broken lines. This analysis suggests an overall RMS coordinate error for this structure determination of 0.18 Å. The top portion of this figure (axes at top and right) shows the fraction of reflections observed and used in refinement as a function of resolution.

Final structural refinement was carried out using a restrained parameter least-squares approach with PROLSQ (Hendrickson, 1985). This involved additional alternating cycles of refinement and manual adjustments based on omit and difference electron density maps covering the full course of the polypeptide chain. As part of this process, an extensive search for bound water molecules was conducted using the ASIR method (Tong et al., 1994), with subsequent manual verification of the significance of the positions identified. All water molecules were refined as neutral oxygen atoms having full occupancy and only those refining to thermal factors smaller than 76 Å^2 were retained in subsequent refinements. Also corrected at this point was the structure of the N-terminal glutamine residue, which was found to be modified posttranslationally to form a stable pyrrolidone derivative.

The final refined structure of human pancreatic α-amylase is composed of 496 amino acids, a calcium ion, a chloride ion, and 360 water molecules. The final crystallographic R-factor obtained was 17.4% and a summary of other refinement results is presented in Table 3. Table 4 provides an analysis of the stereochemistry of the refined human pancreatic α-amylase structure and the restraint weights used. An estimate of 0.18 Å can be made for the overall RMS coordinate error of the current structure based on the Luzzati (1952) plot shown in Figure 9. The coordinates for human pancreatic α-amylase have been deposited in the Protein Data Bank (Bernstein et al., 1977).

Acknowledgments

We thank Robert Besterd and Dr. Joanne Wright of the UBC Health Sciences Center Hospital for assistance in obtaining pancreatic material. X-ray diffraction data were collected on area detectors generously made available by Professor Louis Delbaere (University of Saskatchewan), Professor Daniel Yang (McMaster University), and Dr. Jan Troup (Molecular Structure Corporation). Yili Wang provided technical assistance in protein purification and crystallization. Access to the atomic coordinates for porcine α-amylase by Dr. Steven Larson and Professor Alex McPherson is gratefully acknowledged. This work was supported by an operating grant from the Medical Research Council of Canada (MT-10940).

References

Bernstein FC, Koetzle TF, Williams GJB, Meyer EF Jr, Brice MD, Rodgers JR, Kennard O, Shimanouchi T, Tasumi M. 1977. The Protein Data Bank: A computer archival file for macromolecular structure. *J Mol Biol 112*:535-542.

Bodansky M, Martinez J. 1983. Side reactions in peptide synthesis. In: Gross E, Meienhofer J, eds. *The peptides, vol 5*. New York: Academic Press. pp 111-216.

Boel E, Brady L, Brzozowski AM, Derewenda Z, Dodson GG, Jensen VJ, Petersen SB, Swift H, Thim L, Woldike HF. 1990. Calcium binding in α-amylases: An X-ray diffraction study at 2.1 Å resolution of two enzymes from *Aspergillus*. *Biochemistry 29*:6244-6249.

Brady RL, Brzozowski AM, Derewenda ZS, Dodson EJ, Dodson GG. 1991. Solution of the structure of *Aspergillus niger* acid α-amylase by combined molecular replacement and multiple isomorphous replacement methods. *Acta Crystallogr B 47*:527-535.

Brogard JM, Willemin B, Bleckle JF, Lamelle AM, Stahl A. 1989. Alpha-glucosidase inhibitors: A new therapeutic approach to diabetes and functional hypoglycemia. *Rev Med Interne 10*:365-374.

Brünger AT. 1992. *X-PLOR: A system for X-ray crystallography and NMR*. New Haven, Connecticut: Yale University Press.

Burk D, Wang Y, Dombroski D, Berghuis AM, Evans SV, Luo Y, Withers SG, Brayer GD. 1993. Isolation, crystallization, and preliminary diffraction analyses of human pancreatic α-amylase. *J Mol Biol 230*:1084-1085.

Clissord SP, Edwards C. 1988. Acarbose: A preliminary review of the phar-

macodynamic and pharmacokinetic properties and therapeutic potential. *Drugs 35*:214-243.

Gumucio DL, Wiebauer K, Caldwell RM, Samuelson LC, Meisler MH. 1988. Concerted evolution of human amylase genes. *Mol Cell Biol 8*:1197-1205.

Hendrickson WA. 1985. Stereochemically restrained refinement of macromolecular structures. *Methods Enzymol 115B*:252-270.

Jespersen HM, MacGregor EA, Henrissat B, Sierks MR, Svensson B. 1993. Starch and glycogen debranching and branching enzymes: Prediction of structural features of the catalytic $(\alpha/\alpha)_8$-barrel domain and evolutionary relationship to other amylolytic enzymes. *J Protein Chem 12*:791-805.

Kadziola A, Abe J, Svensson B, Haser R. 1994. Crystal and molecular structure of barley α-amylase. *J Mol Biol 239*:104-121.

Kluh I. 1981. Amino acid sequence of hog pancreatic α-amylase iso-enzyme I. *FEBS Lett 136*:231-234.

Larson SB, Greenwood A, Casio D, Day J, McPherson A. 1994. Refined molecular structure of pig pancreatic α-amylase at 2.1 Å resolution. *J Mol Biol 235*:1560-1584.

Levitzki A, Steer ML. 1974. The allosteric activation of mammalian α-amylase by chloride. *Eur J Biochem 41*:171-180.

Lifshitz R, Levitzki A. 1976. Identity and properties of the chloride effector binding site in hog pancreatic α-amylase. *Biochemistry 15*:1987-1993.

Loyter A, Schramm M. 1962. The glycogen-amylase complex as a means of obtaining highly purified alpha-amylases. *Biochim Biophys Acta 65*: 200-206.

Luzzati V. 1952. Traitement statistique des erreurs dans la détermination des structures cristallines. *Acta Crystallogr 5*:802-810.

MacGregor E. 1988. α-Amylase structure and activity. *J Protein Chem 7*:399-415.

Minamiura N. 1988. Human salivary and pancreatic α-amylases. In: Yamamoto T, Kitahata S, eds. *Handbook of amylases and related enzymes*. Tokyo: Pergamon Press. pp 18-22.

Nakajima R, Imanaka T, Aiba S. 1986. Comparison of amino acid sequences of eleven different α-amylases. *Appl Microbiol Biotechnol 23*:355-360.

Nakamura Y, Ogawa M, Nishide T, Emi M, Kosaki G, Himeno S, Matsubara K. 1984. Sequences of cDNAs for human salivary and pancreatic α-amylases. *Gene 28*:263-270.

Nishide T, Emi M, Nakamura Y, Matsubara K. 1986. Corrected sequences of cDNAs for human salivary and pancreatic α-amylases. *Gene 50*: 371-372.

Pasero L, Mazzei-Pierron Y, Abadie B, Chicheportiche Y, Marchis-Mouren G. 1986. Complete amino acid sequence and location of the five disulfide bridges in porcine pancreatic α-amylase. *Biochim Biophys Acta 869*:147-157.

Qian M, Haser R, Buisson G, Duee E, Payan F. 1994. The active center of a mammalian α-amylase. Structure of the complex of a pancreatic α-amylase with a carbohydrate inhibitor refined to 2.2 Å resolution. *Biochemistry 33*:6284-6294.

Qian M, Haser R, Payan F. 1993. Structure and molecular model refinement of pig pancreatic α-amylase at 2.1 Å resolution. *J Mol Biol 231*:785-799.

Scheppach W, Fabian C, Ahrens F, Spengler M, Kasper H. 1989. Effect of starch malabsorption on colonic function and metabolism in humans. *Gastroenterology 95*:19549-19555.

Semenza G. 1987. Glycosidases. In: Kenny AJ, Turner AJ, eds. *Mammalian ectoenzymes*. B.V. Elsevier Science Publishers. pp 265-287.

Svens E, Kapyaho K, Tanner P, Weber TH. 1989. Immunocatalytic assay of pancreatic alpha-amylase in serum and urine with a specific monoclonal antibody. *Clin Chem 35*:662-664.

Swift HJ, Brady L, Derewenda ZS, Dodson EJ, Dodson GG, Turkenburg JP, Wilkinson AJ. 1991. Structure and molecular model refinement of *Aspergillus oryzae* (TAKA) α-amylase: An application of the simulated-annealing method. *Acta Crystallogr B 47*:535-544.

Takkinen K, Pettersson RF, Kalkkinen N, Palva I, Soderlund H, Kaariainen I. 1983. Amino acid sequence of α-amylase from *Bacillus amyloliquefaciens* deduced from the nucleotide sequence of the cloned gene. *J Biol Chem 258*:1007-1013.

Toda H. 1988. Data on individual amylases. In: Yamamoto T, Kitahata S, eds. *Handbook of amylases and related enzymes*. Tokyo: Pergamon Press. pp 18-75.

Toda H, Konda K, Narita K. 1982. The complete amino acid sequence of Taka-amylase A. *Proc Jpn Acad 58*:208-212.

Tong H, Berghuis AM, Chen J, Luo Y, Guss JM, Freeman HC, Brayer GD. 1994. ASIR: An automatic procedure for determining solvent structure in protein crystallography. *J Appl Crystallogr 27*:421-426.

Truscheit E, Frommer W, Junge B, Muller L, Schmidt DD, Wingender W. 1981. Chemistry and biochemistry of microbial alpha-glucosidase inhibitors. *Angew Chem Int Ed Engl 20*:744-761.

Vallee BL, Stein EA, Sumerwell WN, Fischer EH. 1959. Metal content of α-amylases of various origins. *J Biol Chem 234*:2901-2905.

Wise RJ, Karn RC, Larsen SH, Hodes ME, Gardell SJ, Rutler WJ. 1984. A complementary DNA sequence that predicts a human pancreatic amylase primary structure consistent with the electrophoretic mobility of the common isozyme, Amy_2 A. *Mol Biol Med 2*:307-322.